SCALP ELECTRODE IMPEDANCE, INFECTION RISK, AND EEG DATA QUALITY

Thomas C. Ferree † °

Phan L. Luu † *

Gerald S. Russell † ‡

Don M. Tucker † *

† Electrical Geodesics, Inc., Riverfront Research Park, Eugene, OR

° Computational Science Institute, University of Oregon

* Department of Psychology, University of Oregon

‡ Regena Software, San Diego, CA

Running title: Scalp-electrode impedance and EEG data quality.

Correspondence author: Dr. Thomas C. Ferree, Phone: (541) 687-7962, Fax: (541) 687-7963.

Keywords: Electroencephalography, infection risk, electrode impedance, differential amplifiers, signal loss, 60 Hz noise.

PREPRINT

Submitted to Electroencephalography and Clinical Neurophysiology

Abstract

Objective: Breaking the skin when applying scalp electroencephalographic (EEG) electrodes creates the risk of infection from blood-born pathogens such as HIV, Hepatitis-C, and Crutzfeld-Jacob Disease. Modern engineering principles suggest that excellent EEG signals can be collected with high scalp impedance (≈ 40 kΩ) without scalp abrasion. The present study was designed to evaluate the effect of electrode-scalp impedance on EEG data quality.

Methods: The first section of the paper reviews electrophysiological recording with modern high input-impedance differential amplifiers and subject isolation, and explains how scalp-electrode impedance influences EEG signal amplitude and power line noise. The second section of the paper presents an empirical test of EEG data quality as a function of scalp-electrode impedance for the standard frequency bands in EEG and ERP (event-related potential) recording.

Results: There was no significant change in amplitude of any EEG frequency as scalp-electrode impedance increased from less than 5 kΩ (abraded skin) to 40 kΩ (intact skin). As expected, 60 Hz noise increased linearly as a function of the absolute impedance and impedance mismatch between the measurement and reference electrodes.

Conclusion: With modern high input-impedance amplifiers and accurate digital filters for power line noise, high-quality EEG can be recorded without skin lesions.

Introduction

Before laboratory computers, the quality of the EEG record was dependent on the signal recorded on paper. Noise from power lines (50 or 60 Hz) could not be separated once it was introduced, and the required procedure was to abrade the skin to achieve a scalp-electrode impedance of less than 5 kΩ. To achieve such impedance levels, skin abrasion is required. Abrasion removes the surface epidermal layer, which has higher impedance than the underlying tissue.

Electrode Infection Risk

The primary concern with breaking the skin is infection risk. Once the scalp is abraded, the electrodes or their attachments are likely to contact blood products (Putnam, et al., 1992). Infection with a blood-borne pathogen, such as human immunodeficiency virus (HIV), hepatitis C virus (HCV), or Creutzfeldt-Jacob Disease (CJD), may be unsymptomatic for many years before manifesting as a terminal disease. The United States Center for Disease Control (www.cdc.gov) has issued guidelines for the prevention of blood-born pathogens through disinfection and sterilization of reusable instruments (CDC, 1991; 1993):

(1) instruments that touch intact skin are non-critical and should be disinfected with low-level or intermediate disinfection;

(2) instruments that touch mucous membranes but will not touch bone or penetrate tissue are semi-critical and should be subject to high-level disinfection if they cannot be sterilized;

(3) instruments that touch bone or penetrate tissue are critical and must be sterilized.

Remarkably, sterilization is not adequate to destroy the prion pathogen of CJD (American Electroencephalographic Society, 1984). After intracranial EEG electrodes had accidentally caused transmission of CJD from a demented patient to two younger epileptic patients, the electrodes were implanted in the brain of a chimpanzee. The animal developed CJD within 18 months (Gibbs, et al., 1994).

Thus, when breaking the skin through scalp abrasion EEG electrodes may come into contact with blood products, and it is therefore not adequate to disinfect them, as has been recommended by Putnam et al. (1992). Rather, to meet CDC guidelines, electrodes that contact broken skin

must be sterilized. Current research guidelines recommend not only scalp abrasion but puncturing the skin under each electrode with a surgical lance in order to reduce skin potentials (Picton, et al., 2000). Using a sterile lance is ineffective if the punctured skin is then placed into contact with a non-sterile electrode. Unfortunately, even disinfection of EEG electrodes is but cursory in most research and clinical laboratories.

Spatial Sampling, Application Speed, and Subject Comfort

There are three additional drawbacks to scalp abrasion and skin puncturing. Modern EEG systems are able to record from 128 or 256 scalp sites. Lesioning each site individually may become painful, and it is not uncommon for subjects to refuse EEG recording based upon discomfort. Without recording from sufficient scalp sites, the recording of the brain's electrical field is distorted by spatial aliasing (Srinivasan, et al., 1998). Furthermore, individual site preparation precludes rapid application of an EEG sensor (electrode) array in emergency settings such as in acute stroke assessment. Though certainly important, these factors are secondary in relation to the risk of infection by blood-born pathogens. The following review of modern engineering principles explains why scalp abrasion is no longer necessary.

EEG recording with high input-impedance differential amplifiers

In EEG recordings, electric potential or voltage is measured on the scalp surface, and used to detect and localize the activity of the brain. The definition of electric potential as a physical quantity requires that it always be measured as a difference between two sites. This is accomplished with differential amplifiers. Huhta and Webster (1973) presented a classical electrical engineering analysis of signal loss and 60 Hz noise in electrocardiographic (ECG) recording using differential amplifiers. Our analysis extends theirs in two main ways to make it relevant to modern EEG.

First, Huhta and Webster assumed that the subject was connected to true ground. This simplification reduces the number of variables in the calculations, but it is no longer appropriate. Grounding the subject is unsafe because it increases the risk of electric shock. Modern safety regulations require that the subject must be isolated from ground so that contact with an electric source would not result in the subject creating a path to ground. Furthermore, grounding also allows more 60 Hz noise to enter the measurements. Modern amplifiers use an "isolated

common" electrode which is electrically isolated from the ground of the power supply. In this configuration, the potential of both measurement and reference leads are measured relative to this common electrode and only their difference is amplified. Since the subject is only capacitively coupled to ground, the 60 Hz noise due to electric fields is greatly reduced.

Second, Huhta and Webster assumed the ground electrode was connected to the subject's foot, at maximal distance from the recording and reference electrodes which were located on the torso for cardiac recording. This supports the assumption that the ground electrode is electrically quiet, which is convenient for interpretating the resulting signals. In EEG systems, however, both the reference and common electrodes are usually located on the head in order to minimize 60 Hz common-mode noise sources, as well as noise from ECG signals. In general, nonzero sources of potential difference will exist between each electrode and the common, as well as between the recording and reference electrodes.

Figure 1 shows a circuit diagram for measuring EEG data on the head using a differential amplifier with an isolated common lead.

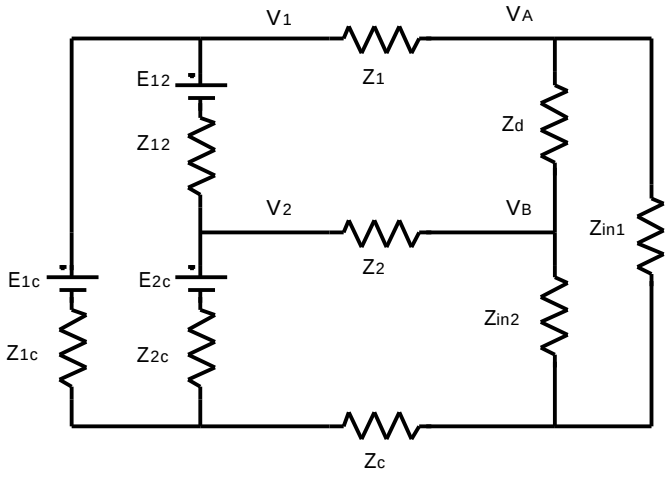

Figure 1. Simplified circuit diagram for understanding the relationship between scalp-electrode impedances and amplifier input impedances.

Z_1 and Z_2 represent the scalp-electrode impedances for recording and reference electrodes, respectively, and Z_c represents the scalp-electrode impedance for the common electrode. Z_{in1} and Z_{in2} represent the amplifier input impedances for recording and reference electrodes, and Z_d represents the amplifier differential input impedance. E_{12}, E_{1c} and E_{2c} represent bioelectric sources located between the designated electrodes. In reality, brain sources are not DC but are

oscillatory and broad-banded. Since the physics of volume conduction in biological tissue is quasi-static, however, at each time point these AC sources may be considered as effective DC sources (Nunez, 1981). Z_{12}, Z_{1c} and Z_{2c} represent the bulk impedance of the head tissue between the designated electrodes. V_1 and V_2 are the scalp potentials just below the scalp-electrode interface, whose difference we are trying to measure, and $V_A - V_B$ is the potential difference measured by the amplifier.

Our first objective is to quantify how $V_A - V_B$ differs from $V_1 - V_2$, as a function of the scalp-electrode impedances. These quantities differ because of current flow into the amplifiers and because of external electric and magnetic fields coupling to the electrode leads and body. As shown below, signal loss depends on the measurement and reference electrode impedances individually, whereas 60 Hz electric noise depends only upon impedance mismatches. For a normal distribution of impedance values, the values and their possible mismatches will be closely related because a distribution of higher impedance values will tend also to have higher mismatches, e.g., a set of scalp-electrodes with 1–5 kΩ impedances will have mismatches of at most about 5 kΩ, while a set with 10–50 kΩ impedances will have mismatches of at most about 50 kΩ. Note also that as sponge electrodes dry the impedances drift to 50–100 kΩ, but if all the electrodes dry together then the mismatches remain of at most about 50 kΩ.

Signal amplitude attenuation

Whenever electric current flows through an impedance there is an associated potential drop. At the scalp-electrode interface, a higher impedance results in a higher voltage drop and some attenuation of signal amplitude. This is a well-known problem which has a standard remedy. By designing amplifiers which have input impedances much higher than the scalp-electrode impedances, the current flow is made low enough that the corresponding potential drop is negligible. Modern EEG amplifiers have input impedances consisting of a resistive component on the order of 200 MΩ in parallel with a capacitive component on the order of 10 pF (corresponding to a reactance of 265 MΩ at 60 Hz). These impedances are very large compared to the scalp-electrode impedance even without scalp abrasion. When using differential amplifiers which amplify the potential difference between two leads, the effect of the scalp-electrode impedance may be either to reduce or increase the potential difference, depending upon

which electrode has higher impedance. This differential signal loss may therefore be more accurately called measurement error.

Using Ohm's law and current conservation on the circuit in Figure 1 leads to nine linear equations for the nine unknown currents in each branch of the circuit. Solving these equations simultaneously leads to an exact expression for the potential difference $V_A - V_B$. To simplify the result, we made following assumptions: First, we assumed that $Z_{12} \approx Z_{1c} \approx Z_{2c}$, which is reasonable in comparison to the scalp-electrode impedances and amplifier input impedances. (Numerical estimates of human head tissue impedances are given below.) Second, we assumed that $Z_d >> Z_{in}$, neglecting the differential amplifier impedance. Third, we assumed that the amplifier input impedances were balanced, i.e., $Z_{in1} = Z_{in2}$, in order to stay focussed on the role of scalp-electrode impedances rather than on amplifier imperfections. To derive a relationship between Z_1,Z_2 and Z_{in} which accounts for their different magnitudes, we expanded the remaining expression for $V_A - V_B$ in a Taylor series keeping only linear terms in the ratios Z_1/Z_{in} and Z_2/Z_{in}. This leads to the following expression for the measurement error:

$$\left(V_A - V_B\right) = \left(V_1 - V_2\right) + \frac{E_{2c}Z_2 - E_{1c}Z_1}{Z_{in}} + O\left(\frac{1}{Z_{in}}\right)^2$$

The left hand side is the potential difference across the two leads as measured by the differential amplifier. The first term on the right hand side is the actual difference in scalp potentials. The second term on the right hand side is a linear estimate of the measurement error as a function of scalp-electrode and amplifier input impedances. The error depends on the source strengths E_{1c} and E_{2c} individually, preventing us from stating the error as a simple percentage of the difference $V_1 - V_2$. Order of magnitude estimates are easily made, however, and can be refined for particular circumstances.

To make numerical estimates, we assumed $Z_{in} \approx 200$ MΩ. Assuming that with scalp abrasion Z_1 and Z_2 are in the range 1–5 kΩ, their maximum ratio with Z_{in} is at most 0.0025%, which is completely negligible. Assuming that without scalp abrasion Z_1 and Z_2 are in the range 10–50 kΩ, their maximum ratio with Z_{in} is 0.025%, which is an order of magnitude larger but *still* completely negligible. More precise statements can be made in particular circumstances. For example, if $E_{1c} \approx -E_{2c}$, as for two electrodes located on opposite sides of a dipolar current source, the error depends upon $Z_1 + Z_2$, approximately twice the average scalp-electrode

impedance. Since $V_1 - V_2$ would be substantial in this case, the percentage error would be very small. In contrast, if $E_{1c} \approx E_{2c}$, as for two nearby electrodes, the error depends upon $Z_1 - Z_2$, the impedance mismatch. Since $V_1 - V_2 \approx 0$ in this case, the percentage error does not vanish. Even in this case, for brain source potentials just under the scalp surface for which $E_{1c} \approx E_{2c} \approx 50$ μV and assuming a maximum impedance mismatch $Z_1 - Z_2 \approx 50$ kΩ, the resulting measurement error would be approximately 0.0125 μV, still far below the desired precision for EEG scalp recordings. Thus signal loss or measurement error is insignificant even without scalp abrasion, provided high input-impedance amplifiers are used.

Environmental sources of 60 Hz noise

AC devices in the recording environment introduce 60 Hz noise into the data. This occurs because electric and magnetic fields incident on the electrode leads and body generate potentials which add linearly to the signal. Huhta and Webster (1973) have considered the sources and effects of 60 Hz noise when using differential amplifiers for ECG, assuming that the subject was connected to true ground. This simplifies their calculations, but increases the risk of electric shock and increases the amount of 60 Hz noise contaminating the recording. The standard practice now is to measure all potentials relative to a dedicated common electrode which is electrically isolated from ground. This improves subject safety and reduces 60 Hz noise. The following discussion emphasizes how the 60 Hz noise amplitude varies as a function of circuit parameters, when using a differential amplifier and an isolated common electrode located on the head.

Magnetic induction

Alternating currents in the recording environment produce time varying magnetic fields. By Faraday's law, a conducting loop will experience an induced potential if oriented properly with respect to the field. For a simple loop of conducting wire, the potential induced across the end of the loop is equal to

$$V_M = 2\pi f A B$$

where f = 60 Hz, A is the loop area and B is the vector component of the 60 Hz magnetic field oriented perpendicular to the loop surface. In ECG, it is usually recommended that the leads be

twisted near the chest before running to the amplifier, minimizing the loop area and reducing magnetic noise. In EEG, the leads are typically bundled near the head before running to the amplifier, and this was the case in our experiments.

The amplitude of the magnetic field B and induced potential V_M depends upon the recording environment. To estimate of the size of V_M in a typical recording environment, we first assumed a magnetic field value equal to that measured by Huhta and Webster (1973): $B = 0.32\ \mu Wb/m^2$. Taking the maximum effective loop area to be one-half the cross-sectional area of a human head with radius r = 9.2 cm gives $A \approx 133\ cm^2$. This leads to $V_M \approx 1.6\ \mu V$, which would be detectable by most EEG amplifiers. The primary contribution to $V_A - V_B$ comes from the current loop formed by the measurement and reference electrode leads and partly the head. Yet with a common electrode located on the head, a potential difference can also be induced magnetically in the two other loops formed by the measurement and reference electrodes with the common electrode. Depending upon how the individual loops are oriented with respect to the field, these contributions may effectively cancel or add. This estimate of the magnetic noise amplitude is consistent with the amount of 60 Hz noise seen in Figure 4, since the analyses below suggest that some portion of the 60 Hz noise in Figure 4 arose from electric coupling. Using a simple loop of wire we measured similar potentials in our environment, and found that 60 Hz magnetic noise increased by an order of magnitude when near the isolation transformer.

Electric displacement currents

Background electric fields also produce 60 Hz noise in bioelectric recordings. This can occur by two similar mechanisms. In the first, the background electric field couples to the electrode leads. In the second, the background electric field couples to the conductive volume of the subject. In either case, it is the 60 Hz potential relative to ground which causes additional currents to flow to ground. While the resulting currents may be similar in each of the three leads, various impedance imbalances produce 60 Hz noise in the difference $V_A - V_B$. We assume here that most electric displacement coupling occurs through the electrode leads.

Figure 2 shows a simplified circuit for understanding the origin of 60 Hz electric noise in EEG recordings by this mechanism. The scalp-electrode impedances and head tissue impedances are represented as in Figure 1, but the EEG source elements are omitted to focus on the 60 Hz signal. The amplifier impedances are assumed to be infinite, which is valid in this

context because the capacitive coupling of the body and amplifier to ground provide the primary current path for 60 Hz currents. We have determined experimentally that for our amplifier system $Z_g \approx 20$ MΩ at 60 Hz, an order of magnitude smaller than the amplifier input impedance Z_{in}. Coupling to the leads is introduced via capacitors, whose values (Z_{d1}, Z_{d2} and Z_{dc}) depend on the dielectric properties of the space between nearby AC devices and the EEG leads. Because these values are difficult to determine independently, following Huhta and Webster (1973), we express the capacitive coupling in terms of the current I_d induced in each lead. Because all three leads run together from the head to the amplifier and subjects are in the near field of the 60 Hz potential, the induced current is likely to be in phase and approximately equal across leads.

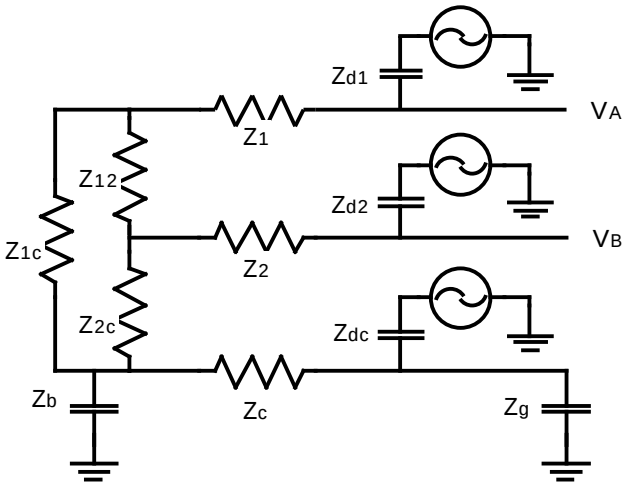

Figure 2. Capacitive coupling of 60 Hz electric noise into scalp electrode leads.

Using Ohm's law and current conservation on the circuit in Figure 2 leads to the following equation for the amplitude of 60 Hz noise due to capacitive coupling

$$V_E = I_d(Z_2 - Z_1) + I_d\left(\frac{Z_{12}(Z_{1c} - Z_{2c})}{Z_{12} + Z_{1c} + Z_{2c}}\right)$$

Both terms are proportional to the induced current I_d. The first term depends only on the scalp-electrode impedance imbalance between measurement and reference electrodes, while the second depends only on the impedances of the conducting head volume.

Huhta and Webster estimated I_d = 6 nA when grounding the subject in a typical recording environment. Displacement currents are substantially reduced, however, by the use of an isolated common electrode rather than a direct subject-ground connection. In Figure 2, Z_{d1}, Z_{d2} and Z_{dc} represent distributed capacitances from diffuse 60 Hz noise sources to the two input cables and amplifier, respectively, while Z_b and Z_g represent distributed capacitances from the subject and amplifier to ground. Typically these impedances are all high and relatively symmetrical. Displacement currents are caused only by asymmetrical coupling into and out of the various components of the system. Assuming that all of the 60 Hz noise in Figure 4 is due to this mechanism provides an upper limit on the electric displacement current $I_d \approx 0.6$ nA in our recordings.

The second term in the above equation explains why there tends to be more 60 Hz noise when the measurement electrode is located near the common electrode, a phenomenon well-known to EEG researchers. The second term is largest when Z_{1c} is very different from Z_{2c}, and vanishes when Z_{1c} is equal to Z_{2c}. The head impedances Z_{ij}, which appear in the second term, are difficult to measure independently in living humans, but can be estimated using computer simulations of volume conduction through biological tissue and assuming standard radii and conductivity values for the human brain, CSF, skull and scalp (Rush and Driscoll, 1969; Ferree et al., 2000). We have done this in computer simulation by injecting current through a pair of electrodes and calculating the potentials at the underlying scalp locations. We assumed the electrodes to be 1 cm in diameter, and that the injected current is distributed uniformly over its surface area. (In reality, most current flows along the outer edge of the electrode (Wiley and Webster, 1982), but this effect has little effect on the potentials over distances large compared to the electrode diameter.) Within these approximations, we find head impedance values ranging 300 – 500 Ω, depending upon the distance between the injection electrodes and the choice of skull conductivity. The location of the reference and common electrodes are usually fixed. Assuming $Z_{1c} \approx Z_{12} \approx Z_{2c}$, as when the electrodes are evenly distributed over the head, this term makes no contribution. Assuming $Z_{1c} \approx 300$ Ω and $Z_{12} \approx Z_{2c} \approx 500$ Ω, as when the measurement electrode is located near the common electrode, and assuming the induced current $I_d \approx 0.6$ nA, we estimate $V_E \approx 5$ μV for the second term, which is similar to what is observed experimentally.

Methods and Materials

Measurement of scalp-electrode impedance

To quantify the dependence of EEG signal quality on scalp-electrode impedance, we need to be able to measure scalp-electrode impedances accurately. Ideally, this would be done by passing a known current across the scalp-electrode interface, and measuring the potential difference between points just above the electrode and just below the scalp. Since making an independent measurement of the potential just below the scalp surface is impractical, an approximate method is required. Figure 3 shows a circuit diagram for this purpose. Only four electrodes are shown, when in practice there would be 20, 130, etc. Z_1 through Z_4 represent the four scalp-electrode impedances in a configuration for measuring impedance Z_4. The head impedances are shown, but are omitted from the calculations below since they are small compared to the scalp-electrode impedances. This particular approximation is more valid without scalp abrasion.

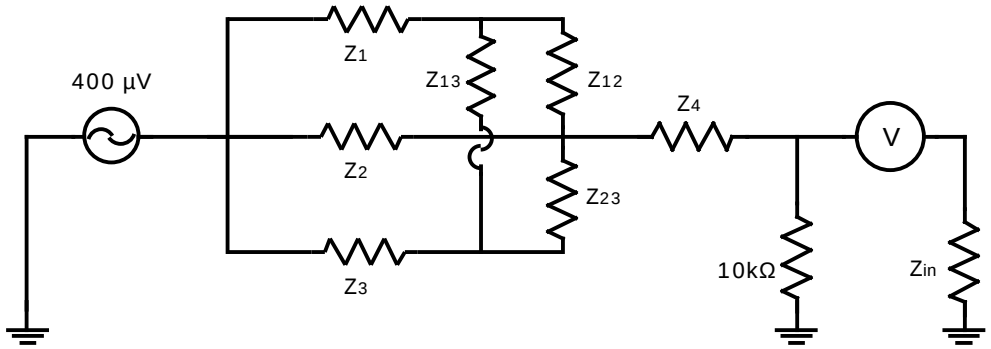

Figure 3. Circuit configuration for measuring scalp-electrode impedances.

A simple method for measuring the scalp-electrode impedance Z_4 is based on the fact that, when K similar resistors ($Z_1 \approx Z_2 \approx \ldots \approx Z_K$) are connected in parallel, they have an effective resistance which is smaller according to the formula

$$\frac{1}{Z_{eff}} = \frac{1}{Z_1} + \frac{1}{Z_2} + \ldots + \frac{1}{Z_K} \approx \frac{K}{Z_1}$$

Thus by driving all but one of the electrodes to a known potential relative to ground (400 μV), the potential at the scalp will be very nearly equal to the known potential. For K sufficiently large, the error in such an approximation may be estimated by the addition of one term, or 1/K. For a 128-channel amplifier, K=128-1 and the error is approximately 1/(128-1) or 0.79%, and to a very good approximation it is as though the impedance Z_4 is connected directly the 400 μV source. The remaining circuit is a simple voltage divider, and by measuring the potential V the value of Z_4 is given by

$$Z_4 = \frac{10\text{k}\Omega\,(400\mu\text{V} - \text{V})}{\text{V}}$$

The amplitude V must be determined from the oscillatory signal. This is simple, but takes some computer time for many channels. A faster but more approximate algorithm drives all but six electrodes at a time, and measures these six scalp-electrode impedances simultaneously. The error in this approximation is slightly larger. Since the same current flows in parallel through the six electrodes the error is roughly 6/(128-6) or 4.9%. This latter method was used to measure the scalp-electrode impedances in the present experiments.

Subjects

In order to provide experimental verification of the engineering principles discussed above, we collected EEG data from ten normal subjects from electrodes with and without scalp abrasion, with impedances that varied from < 5 kΩ to 40 kΩ. We tested for loss of signal amplitude at all standard EEG frequencies and at 60 Hz. All procedures were approved by the EGI (Electrical Geodesics, Inc.) Human Subjects Institutional Review Board.

EEG data collection

EEG data was recorded using the Geodesic Sensor Net (Tucker, 1993), which arranges 129 Ag/AgCl electrodes in a tension structure that insures the sensors are distributed evenly across the head surface. The EEG signal was amplified with a high input-impedance (200 MΩ) Net Amps dense-array amplifier (Electrical Geodesics, Inc., Eugene, Oregon). The data were recorded with a 0.1 to 100 Hz analog band-pass filter and digitized at 250 s/sec with a 16-bit analog-to-digital

converter. The data were collected with the common electrode located on the nasion and the referenced electrode located at the vertex.

The impedances of the reference and a single measurement channel were systematically and independently varied. The measurement channel was located over the right occipital region, because a strong biological signal (alpha) can be clearly identified. When the Geodesic Sensor Net was applied with saline-sponge electrodes, the scalp-electrode impedances were approximately 10 kΩ. Lower impedance values were obtained by abrading the scalp with a ground glass preparation (Omni Prep, D. O. Weaver and Co.). Higher impedance values were obtained by wicking saline away from the sponge electrode (simulating the drying that occurs over three hours of recording). Once the desired impedance levels for the reference and measurement electrodes were obtained, two minutes of eyes-closed, resting EEG were acquired for each subject.

Fourier spectral analysis

For each subject and condition, five 10-second epochs of EEG were selected for their lack of obvious artifacts. Each epoch was divided into ten 1-second segments, multiplied by a Hanning window to reduce bin-width artifacts, and Fourier transformed using a standard FFT algorithm. The resulting power spectra had 1 Hz frequency resolution, and were expressed as frequency-domain spectral amplitudes by taking the modulus of the appropriate Fourier coefficients. The amplitudes were normalized so that an integer-frequency sine wave with a 1 uV peak amplitude in the time domain would result in a 1 uV amplitude in the frequency domain. The fifty amplitude spectra from all five epochs were then averaged to reduce the variance arising from the natural fluctuations in the EEG power spectrum.

We defined delta (1-3 Hz), theta (4-7 Hz), alpha (8-12 Hz), beta (13-40 Hz) and ambient noise (59-61 Hz) bands for individual analyses. Figure 4 superimposes the amplitude spectra for each impedance condition from a representative subject. An alpha peak at 11 Hz and a noise peak at 60 Hz are clearly identifiable.

Statistical analysis

Four impedance levels were defined: 1) <10 kΩ, 2) 11-20 kΩ, 3) 21-30 kΩ, and 4) 31-40 kΩ. This produced a two-factor, completely crossed, within subject design with 16 cells: reference electrode (4 levels) x measurement electrode (4 levels). The amplitude in each frequency band was

statistically analyzed using a repeated measures ANOVA, with reference and measurement channel impedance as the two within-subjects factors.

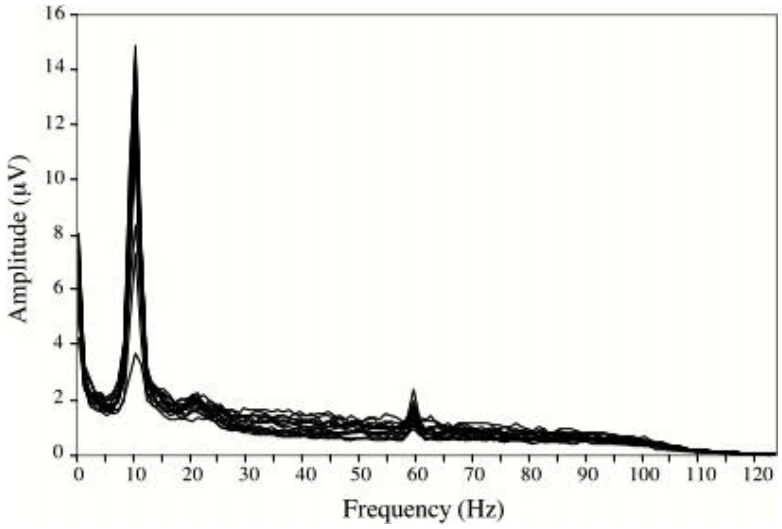

Figure 4. EEG power spectra showing alpha peak and 60 Hz noise.

Results

Table 1 shows the average and standard deviation (in parentheses) of the impedance values for each ANOVA cell. The first row shows the impedance ranges for the reference electrode, and the second row shows the measured values. The first column shows the impedance ranges for the measurement electrode. The last four rows show the impedance values for the measurement electrode, corresponding to each range for the reference electrode.

Reference	<10	11-20	21-30	31-40
	5.5 (1.9)	13.4 (1.6)	24.0 (2.6)	33.6 (2.3)
Measurement				
<10	8.2 (1.2)	7.5 (1.2)	7.2 (1.9)	8.5 (1.1)
11-20	13.0 (2.4)	13.6 (2.6)	14.2 (2.7)	13.9 (3.0)
21-30	22.5 (2.1)	23.1 (2.7)	24.3 (3.2)	25.9 (2.5)
31-40	34.2 (2.7)	35.0 (2.7)	35.4 (3.2)	35.4 (2.9)

Table 1. Scalp-electrode impedance values (kΩ) for reference and measurement electrodes.

The results of the repeated measures ANOVA are discussed below for each frequency band. In each band, the amplitude was considered first as a function of reference and measurement electrode impedance. Because measurement error and 60 Hz noise depend on impedance mismatch, interactions were also considered in the ANOVA.

Delta

Amplitude in the delta band did not vary significantly as a function of reference or measurement electrode impedance: $F(3,27) < 1$ for both factors. The interaction between reference and measurement lead impedance also did not produce significant differences: $F(3,27) < 1$.

Theta

Amplitude in the theta band did not vary significantly as a function of reference lead impedance: $F(3,27) < 1$, or measurement lead impedance: $F(3,27) = 1.3$, $p < 0.3$. The interaction between reference and measurement lead impedance also did not produce significant differences: $F(3,27) < 1$.

Alpha

Amplitude in the alpha band did not vary significantly as a function of reference lead impedance: $F(3,27) < 1$, or measurement lead impedance: $F(3,27) = 1.2$, $p < 0.3$. The interaction between reference and measurement lead impedance also did not produce significant differences: $F(3,27) < 1$ (see Figure 5).

Beta

Amplitude in the beta band did not vary significantly as a function of reference or measurement electrode impedance, $F(3,27) < 1$ for both factors. The interaction between reference and measurement lead impedance also did not produce significant differences: $F(3,27) < 1$.

60 Hz Noise

Figure 5 shows the amplitude in the 60 Hz noise and alpha bands (for comparison) as a function of scalp-electrode impedance. The amplitude in the alpha band (left) does not show a consistent trend with impedance. The amplitude in the 60 Hz noise band (right) did increase as a function of impedance, as predicted, but this effect did not reach statistical significance: $F(3,27) = 1.97$, $p < 0.15$ (reference lead impedance), and $F(3,27) = 1.4$, $p < 0.27$ (measurement lead impedance), or interactions: $F(3,27) < 1$ for the number of subjects and trials used here.

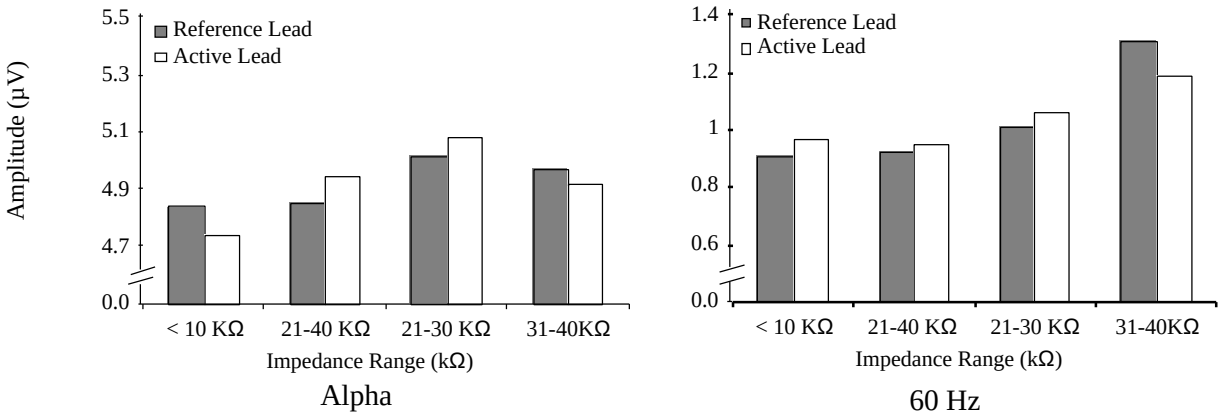

Figure 5. Amplitudes (μV) as a function of reference and measurement electrode impedance..

Figure 6 shows the amplitude in the 60 Hz noise band as a function of impedance mismatch. The small mismatch condition was defined as the set of cases for which the reference and measurement leads were in the same range (e.g., both <10 kΩ). The large mismatch condition was defined as the set of all cases for which the reference and measurement lead impedances were in different and non-neighboring ranges (e.g., when one electrode impedance was <10 kΩ or 11–20 kΩ and the other electrode impedance was 31–40 kΩ. The amount of 60 Hz noise increases with the impedance mismatch, as predicted, but the increase is modest (≈8%).

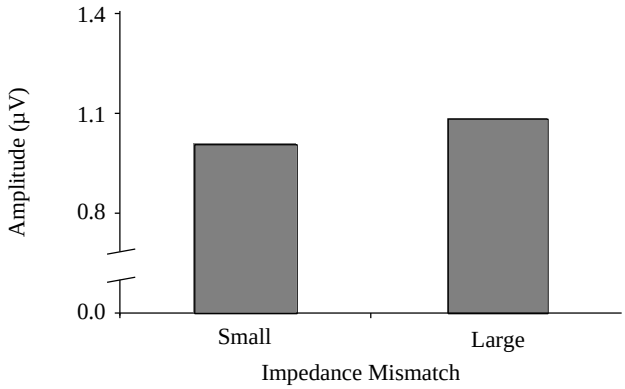

Figure 6. Amplitude in the 60 Hz noise band for small and large impedance mismatch conditions.

Discussion

Scalp abrasion is not necessary for accurate EEG and ERP recording. Concerns about differential signal loss or measurement error are easily resolved by understanding the relation between scalp-electrode impedance and the input-impedance of modern differential amplifiers. If the amplifier input-impedance is high enough, basic circuit analysis predicts that there is a negligible reduction in signal amplitude when using electrodes without abrasion. In our experiments, using an amplifier with an input-impedance of 200 MΩ and scalp-electrode impedances up to 40 kΩ, we demonstrated that there was no significant amplitude reduction or measurement error in any of the EEG frequency bands. Although we did not test the signal quality for scalp-electrode impedances above 40 kΩ in this study, the engineering analysis shows that scalp-electrode impedances up to 200 kΩ still allow for accurate (< 0.1% error) signal acquisition.

Engineering analysis also shows that 60 Hz noise due to magnetic induction may be measurable, but does not depend on the scalp-electrode impedances. In contrast, 60 Hz noise due to electric coupling does increase as a function of scalp-electrode impedance mismatch. This was seen visually in the data, although the effect did not reach statistical significance in this study. We suggest that much of the concern over 60 Hz noise is anachronistic: a holdover from the days of paper recording in which the line noise could not be easily removed from the signal. Although 60 Hz noise is admittedly a distraction when viewing data in real time, its presence is not a practical concern for digital EEG, provided the biological signal of interest is not within 1

or 2 Hz of the 60 Hz frequency band. With digital signal processing, a 60 Hz notch filter cleanly removes this noise from the data.

Skin potentials can only be avoided by puncturing the skin under the electrode. With modern signal analytic methods, it is unikely that skin potentials will be confused with the coherent neural electrical fields measured with a dense sensor array. However, if avoiding skin potentials with a sparse array is desired, sterile electrodes, and not just sterile lances, must be used.

In conclusion, sound engineering principles and empirical tests verify that excellent EEG can be obtained without scalp abrasion. This conclusion is not limited to the Geodesic Sensor Net or Electrical Geodesics products. It applies to any electrode design with good electrochemical and mechanical qualities and any modern differential amplifier with high input impedance. Because of the significant infection risk and inconvenience, scalp abrasion is no longer acceptable in research or clinical practice.

Acknowledgements

The authors gratefully thank Dennis Rech and Tom Renner and for helpful discussions, and Mary Lyda for assistance collecting the data. This work was supported by NIH grants R44-HL-60478, R44-AG-17399 and R44-NS-38829.

References

American Electroencephalographic Society Infectious Diseases Committee Report (1984). Journal of Clinical Neurophysiology 1: 437-41.

American Electroencephalographic Society (1994). Report of the Committee on Infectious Diseases. Journal of Clinical Neurophysiology 11: 128-32.

Ferree, T. C., K. J. Eriksen and D. M. Tucker (2000). Head tissue conductivity estimation for improved EEG analysis. IEEE Transactions on Biomedical Engineering, in press.

Gibbs, C. J., Jr., Asher, D. M., Kobrine, A., Amyx, H. L., Sulima, M. P., & Gajdusek, D. C. (1994). Transmission of Creutzfeldt-Jakob disease to a chimpanzee by electrodes contaminated during neurosurgery. J of Neurol Neurosurg Psychiatry 57: 757-758.

Huhta, J. C. and J. G. Webster (1973). 60-Hz interference in electrocardiography. IEEE Transactions on Biomedical Engineering 20: 91-101.

Nunez, P. L. (1981). Electric fields of the brain: the neurophysics of EEG. Oxford University Press.

Oken, B. S. (1986). Filtering and aliasing of muscle activity in EEG frequency analysis. Electroencephalography and Clinical Neurophysiology 64: 77-80.

Picton, T. W., & al., e. (2000). Guidelines for using human event-related potentials to study cognition: Recording standards and publication criteria. Psychophysiology, 37, 127-152.

Putnam, L. E., Johnson, R., Jr., & Roth, W. T. (1992). Guidelines for reducing the risk of disease transmission in the psychophysiology laboratory. SPR Ad Hoc Committee on the Prevention of Disease Transmission. Psychophysiology, 29(2), 127-141.

Rush, S. and D. A. Driscoll (1969). EEG electrode sensitivity - an application of reciprocity. IEEE Transactions on Biomedical Engineering 16(1): 15-22.

Srinivasan, R., D. M. Tucker and M. Murias (1998). Estimating the spatial nyquist of the human EEG. Behavior Research Methods, Instruments, and Computers 30: 8-19.

Tam, H. W. and J. G. Webster (1977). Minimizing electrode motion artifact by skin abrasion. IEEE Transactions on Biomedical Engineering 24: 134-139.

Tucker, D. M. (1991). Spatial sampling of head electric fields: The geodesic sensor net. Electroencephalography and Clinical Neurophysiology 79: 413-419.

Wiley, J. D. and J. G. Webster (1982). Analysis and control of the current distribution under circular dispersive electrodes. IEEE Transactions on Biomedical Engineering 29(5): 381-385.